An analytical study on the stress-strain relation of PVA-ECC under tensile fatigue

K. Kakuma, T. Matsumoto. T. Hayashikawa & X. He
Hokkaido University, Sapporo, Japan

ABSTRACT: This study proposes the stress-strain relationship of Engineered Cementitious Composite reinforced with polyvinyl alcohol fibers (PVA-ECC) under tensile fatigue. The mechanism of fatigue degradation of ECC is bridging stress degradation on crack plane, and the degradation is modeled in bridging law by introducing the change of micromechanical parameters. In this study, fiber fatigue rupture is regarded as a degradation factor, and the criterion of fiber fatigue rupture dependent on number of cycles is applied. From the calculated bridging stress-crack opening displacement relationship, it is shown that multiple cracking criterion can be satisfied up to a certain number of fatigue cycles. In order to obtain the stress-strain relationship, the bridging stress-crack opening displacement relationship is introduced into finite element analysis as discrete crack model. The estimated evolution of stress degradation agrees well with the evolution obtained from uniaxial tensile fatigue test of PVA-ECC, showing the validity of the current study.

1 INTRODUCTION

Engineered Cementitious Composite (ECC) is one kind of Ductile Fiber Reinforced Cementitious Composite, which shows pseudo strain hardening behavior under uniaxial tension, and has high tensile strain capacity. ECC also shows the effect of crack opening displacement control as the value is defined to be less than 0.2mm (JSCE 2007). In addition, the reduction of fatigue strength is smaller, and the fatigue durability is higher than normal concrete or conventional fiber reinforced cementitious composite, which are strain softening type materials, due to multiple fine cracks. From these characteristics, ECC is expected to be applied to infrastructures as a repair or reinforcement material such as overlay or underlay of bridge slabs, in which fatigue degradation caused by repeated traffic load becomes a significant problem.

In the material design of ECC, micromechanics and fracture mechanics can explain the static property (Li 1993). It is possible to optimize the material design by a parametric study. Fatigue design of material or structures, however, is considered based on static load carrying capacity. Recently, some studies on fatigue have been performed, and the fatigue property of ECC or structure with ECC, such as the mechanism of fatigue degradation of ECC and the effect of reinforcement with ECC, has been revealed. Flexural fatigue test of ECC beams (Matsumoto et al. 2003) and a wheel trucking test of ECC-steel composite deck (Mitamura et al. 2006) are examples of them. However, most studies on fatigue are based on experiment, and a fatigue model of ECC is not sufficiently developed.

The mechanism of fatigue degradation of ECC is the degradation of stress transferred by fibers on crack plane. From the point of development of fatigue design method, the proposition of fatigue model of ECC considering the degradation mechanism and fatigue life prediction method are necessary.

Therefore, this study develops the stress-strain relationship of ECC under tensile fatigue. The concept of fiber bridging stress degradation is based on micromechanics, and the changes of micromechanical parameters due to fatigue are introduced. The stress-strain relationship is obtained by applying the bridging stress degradation model to finite element analysis. From the derived relationship, the evolution of stress degradation is discussed by comparing with uniaxial fatigue tension test of polyvinyl alcohol fiber reinforced ECC (PVA-ECC) conducted by Matsumoto et al. (2004).

2 BRIDGING STRESS DEGRADATION

ECC is designed based on micromechanics, which is the mechanical model formulating the behavior of the components of composites. Bridging law, the relationship between bridging stress and crack opening displacement, is an important relationship, and it can estimate the tensile property of ECC such as tensile strength, fracture energy, cracking state, etc. Fatigue degradation of ECC is caused by the degradation of

bridging stress, and it also can be estimated in bridging law. In this chapter, bridging stress degradation is modeled based on bridging law.

2.1 Bridging law

Bridging law of fiber reinforced cementitious composites is obtained from micromechanical parameters about properties of fiber, matrix and fiber-matrix interface. The typical relationship before pre-peak is shown in Figure 1. For example, maximum bridging stress and the area under bridging stress curve correspond to tensile strength and fracture energy of composites, respectively.

The initiation of pseudo strain hardening behavior of ECC, the unique post-cracking behavior, is also estimated by bridging law as shown in the following (Li. 1993).

$$\sigma_{peak} \geq (\sigma_{fc})_i \tag{1}$$

$$J'_b / J_{tip} \geq 1 \tag{2}$$

where σ_{peak}=maximum bridging stress; $(\sigma_{fc})_i$=crack strength; J'_b=complementary energy of the relationship between bridging stress and crack opening displacement; and J_{tip}=fracture toughness of matrix at crack tip

Equation 1 is the criterion for stress increase after crack initiation, meaning that maximum bridging stress of composites must be larger than crack strength in order to obtain the strain hardening behavior.

Equation 2 is the criterion to obtain steady state cracking, the unique process of crack propagation. Under steady state cracking, cracks propagate with constant crack opening displacement under constant loading, and the initiation of multiple cracks is promoted because bridging stress is retained although crack length becomes large.

Bridging law in this study is a numerical model derived from Fiber Pullout Model (Li. 1992), which is the basic mechanical model of short fiber reinforced composites. In the following sections, the numerical model is explained.

2.1.1 Fiber Pullout Model
Fiber Pullout Model is the mechanical model, which formulates the fiber pullout behavior from matrix derived based on the following assumptions.
- Fibers are 3-D randomly distributed in location and orientation.
- Debonding between fiber and matrix occurs at the side of crack, and progress to the side of embedment.
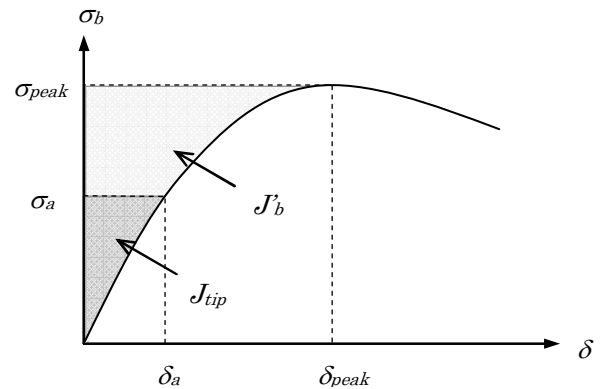
Figure 1. Bridging stress-crack opening displacement relationship before peak.

- The interfacial bond between fiber and matrix is subjected to frictional bond.
- The deformation of matrix is small enough compared with the slip of fibers so that it can be neglected.
- The effect of Poisson's ratio of fiber is neglected, and the elastic modulus of fiber is considered to be constant.
- Fiber rupture does not occur because fiber tensile strength is larger than axial stress.

These assumptions are for cementitious composites reinforced with nylon fibers or polypropylene fibers. Some of them should be expanded, depending on fiber properties for reinforcement. Here, some are expanded by assuming PVA fibers.

2.1.2 Interfacial bond strength
Interfacial bond between fiber and matrix is classified into two kinds: chemical bond and frictional bond (Kanda et al. 1998a). Large chemical bond strength is the specific characteristic of PVA fiber. In this study, the process of the change of interfacial bond, debond of chemical bond and the transition to frictional bond, is defined as a function of relative slip of fibers.

$$\tau = \tau_s [1 - \{1 - (\delta / \delta_{0\tau})\}^2] \quad \text{for } 0 \leq \delta \leq \delta_{0\tau}$$
$$\tau = \tau_i + (\tau_s - \tau_i) Exp[\alpha_\tau \{1 - (\delta / \delta_{0\tau})\}] \quad \text{for } \delta_{0\tau} < \delta \tag{3}$$

where τ=fiber-matrix interfacial bond strength; τ_s=chemical bond strength; τ_i=frictional bond strength; and $\delta_{0\tau}, \alpha_\tau$=parameters $\delta_{0\tau}$ is relative slip when debond of chemical bond starts, and α_τ determines the slop of the transition of chemical bond to frictional bond.

2.1.3 Fiber rupture
For PVA-ECC, fiber rupture must be taken into account because fiber tensile strength is relatively small compared with interfacial bond strength between fiber and matrix. The bridging stress is calculated by the summation of pullout stress transferred

by each fiber with considering the randomness of fiber position and inclining angle.

$$\sigma_b = V_f \int_{\phi=0}^{\pi/2} \int_{z=0}^{(L_f/2)cos\phi} \frac{P}{A_f} p(\phi)p(z)dzd\phi \quad (4)$$

where σ_b=bridging stress; P=pullout load transferred by each fiber; $p(z)$=probability about fiber location; $p(\phi)$=probability about fiber inclining angle; V_f=fiber volume fraction; and A_f=cross section area of fiber-Fiber rupture occurs when axial stress of fibers reaches fiber tensile strength, and the ruptured fibers are removed from Equation 4.

2.1.4 *Fiber strength reduction*
For fibers embedded into matrix, the strength decreases due to the abrasion of fiber surface and bending effect (Kanda et al. 1998a). This apparent strength reduction is expressed by the following equation.

$$\sigma_{fu} = \sigma^n{}_{fu} e^{-f'\phi} \quad (5)$$

where, σ_{fu}=apparent fiber strength; $\sigma^n{}_{fu}$=nominal fiber strength; f'=reduction factor of fiber strength; and ϕ=fiber inclining angle

2.1.5 *The bridging stress-crack opening displacement relationship*
Figure 2 (number of cycles=1) is the relationship between bridging stress and crack opening displacement obtained from the above model. The relationship can reproduce the relationship derived by Kanda et al. (1998b). The differences between this study's model and Kanda's model are treatment of interfacial bond strength and elastic modulus of matrix. For the former, parameters in Equation 3 are determined based on Kanda's model. For the latter, the matrix property can be neglected because the deformation of matrix is sufficiently small due to the ratio of elastic modulus between fiber and matrix.

2.2 *Degradation relation of single fiber*

Fatigue degradation of ECC is caused by bridging stress degradation, and it is caused by fiber fatigue rupture and fiber pullout from matrix. The dominant factor changes, depending on the property of fiber for reinforcement (Matsumoto et al. 2003). More ruptured fibers are observed than pullout fibers in the case of PVA-ECC with relatively low fiber tensile strength compared with interfacial bond strength. On the other hand, the number is opposite in the case of polyethylene fiber reinforced ECC with relatively high fiber tensile strength compared with interfacial bond strength.
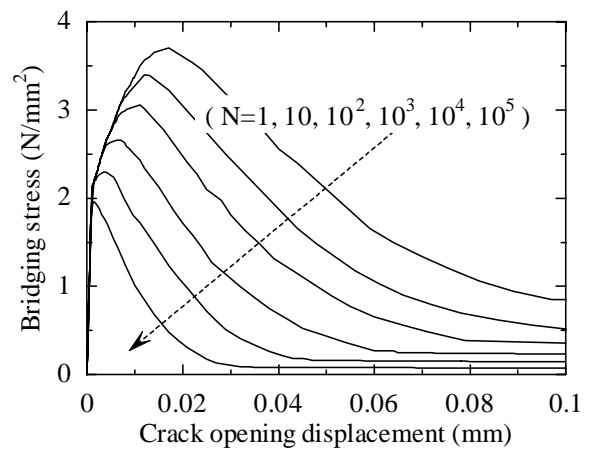
Figure 2. Bridging stress-crack opening displacement under fatigue.

In bridging law, degradation factors can be mod-eled by the change of micromechanical parameters. In micromechanical parameters, the change of fiber tensile strength and interfacial bond strength express fiber fatigue rupture and fiber pullout from matrix, respectively. In the proposed model, only fiber fatigue rupture is considered as a fatigue degradation factor, and the change of fiber tensile strength, which depends on number of cycles, is introduced into bridging law, assuming PVA-ECC (Kakuma et al. 2009a,b).

The criterion of fiber fatigue rupture is represented by the following equation as a function of number of cycles.

$$\frac{\sigma^i{}_N}{\sigma^n{}_{fu}} = 1 - k_f \log(N) \quad (6)$$

where $\sigma^i{}_N$=fiber tensile strength at Nth cycle; $\sigma^n{}_{fu}$=initial fiber tensile strength; k_f=parameter; and N=number of cycles

Fatigue property of PVA fibers has not been sufficiently revealed because the fatigue test of single fiber is difficult. Here, the parameter, k_1, is determined as referring to the S-N diagram of metals as fibers rupture at 100,000 cycles under the stress ratio of 0.5.

2.3 *The bridging stress-crack opening displacement relationship under fatigue tension*

Figure 2 shows the relationship between bridging stress and crack opening displacement under variable number of cycles, N=1, 10, 10^2, 10^3, 10^4 and 10^5. In the figure, bridging stress deteriorates when number of cycles increases. In the relationship before maximum bridging stress, bridging stress degradation is not shown. Figure 2 is a relationship when only fiber strength is a variable parameter in the summation of fiber pullout stress in Equation 4, and the number of ruptured fiber does not change at

the range of small crack opening displacement with the small fiber pullout stress.

Figure 3 is the relationship between the value of J'_b/J_{tip} and number of cycles, which estimates the limit of showing multiple cracking property. In the calculation of the figure, the value of J_{tip}, 3.1kJ/m^2, is constant without regard to number of cycles because the change of fracture toughness of matrix is not applied. The following about tensile behavior under fatigue is suggested when paying attention to the criterion of steady state cracking defined in Equation 2. The strain hardening behavior can be obtained although bridging effect deteriorates due to the increase of ruptured fibers because Equation 2 is satisfied before number of cycles reaches 1,000. Especially before 10 cycles, multiple cracks saturates because the J'_b/J_{tip} value is larger than 3.0, the critical value to show saturated multiple cracking. When the J'_b/J_{tip} value approaches the critical value, $J'_b/J_{tip}=1$, with increase of number of cycles, it is difficult to obtain multiple cracking property. After number of cycles is over 1,000, the localization of particular crack without showing multiple cracking probably occur as same as shown in general short fiber cementitious composites.

3 UNIAXIAL TENSILE FATIGUE TEST

In order to show the validity of the stress-strain relationship under tensile fatigue proposed in this study, the analytical result is compared with uniaxial tensile fatigue test of PVA-ECC conducted by Matsumoto et al. (2004). In this chapter, the summary and the result are explained.

3.1 *Material and test specimen*

Static and fatigue tensile test were conducted for PVA-ECC. The mix proportion of the ECC and the properties of PVA fibers are shown in Table 1 and 2, respectively.

The shape of specimens is shown in Figure 4. Three specimens and nine specimens were prepared for static loading and fatigue loading test, respectively.

3.2 *Loading procedure*

Both static and fatigue loading were conducted under displacement control. The uniaxial tensile tests were conducted under static loading condition before fatigue loading. The static tensile strength and the strain capacity before localization of ECC were determined. Based on the tensile strain capacity from the static test, three levels of maximum tensile strain levels were assigned for fatigue specimens.
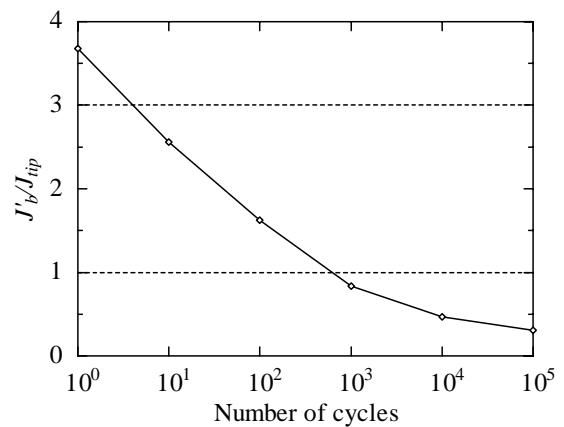
Figure 3. The J'_b/J_{tip} value-number of cycles relationship.

Table 1. Mix proportion of ECC.

Water	1
Cement	0.32
Fine aggregate	0.42
Super plasticizer	0.03
Methylcellulose	0.00071

Table 2. Properties of PVA fibers.

Length (mm)	12
Diameter (μm)	37.7
Volume fraction (%)	2.1
Elastic modulus (kN/mm^2)	36.7
Fiber tensile strength (N/mm^2)	1610
Interfacial bond strength (N/mm^2)	2.01
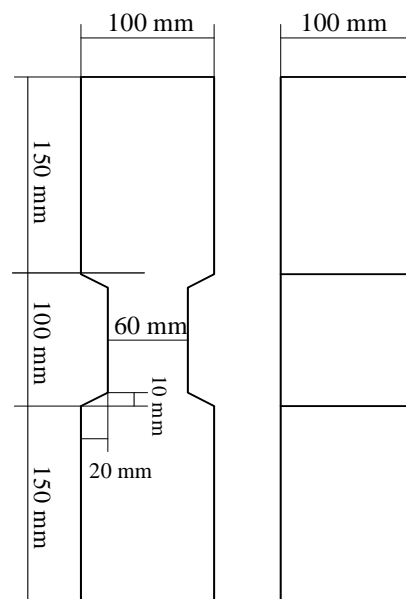
Figure 4. The size of test specimen.

The selected maximum tensile strain levels were 0.01, 0.015 and 0.02, and three specimens were conducted for each tensile strain level.

The uniaxial tensile fatigue tests were performed under strain control condition. Specimens were subjected to a 4Hz sinusoidal cyclic loading. The test was conducted with constant amplitude between maximum tensile strain and minimum tensile strain.

Maximum number of cycles in fatigue loading was 200,000 cycles.

3.3 Test results

3.3.1 Static test

From the uniaxial tensile tests, the unique tensile behavior of ECC, tensile strain increases with repeated stress increase and decrease, was observed. After that, crack localization occurred when tensile strain equals to 0.004. This value tends to be small compared with other uniaxial tensile tests of PVA-ECC with similar fiber property and mix proportion. However, it is regarded that this test has no problems as a compared experiment because multiple cracking and strain hardening behavior after initial cracking were observed.

3.3.2 Fatigue test

In the uniaxial tensile fatigue test, tensile stress gradually reduced at low fatigue loading cycles, and the rate of stress reduction increased when number of cycles increased. Furthermore, the tensile stress of ECC tended to be constant or nearly constant when the number of cycles was in the range of between 100,000 and 500,000 cycles, depending on the maximum tensile strain level. From the evolution of tensile stress after 100,000 cycles, it was suggested that PVA fibers have fatigue limit as shown in metals.

On the observed crack plane after fatigue loading, the number of ruptured fiber was larger than pulled out fibers, and fiber fatigue rupture was the dominant mechanism of fatigue degradation of ECC.

4 THE STRESS-STRAIN RELATIONSHIP UNDER TENSILE FATIGUE

There are two methods to represent crack behavior in finite element analysis: discrete crack model and smeared crack model. The former can directly consider the property of crack such as crack opening displacement and crack length by introducing joint elements at crack location. The latter treats cracked elements as continuous elements even after cracking by assuming that crack distributes a whole element. Bridging stress degradation relationship proposed in the previous chapter is the relationship on crack plane, meaning that it is based on the concept of discrete crack model when applied to finite element analysis. Therefore, the stress-strain relationship under fatigue obtained from bridging stress degradation is beneficial to perform fatigue analysis of ECC as members or structures. In this chapter, the stress-strain relationship under tensile fatigue is derived, and the validity is discussed by comparing with uniaxial tensile fatigue test of PVA-ECC shown in chapter 3.
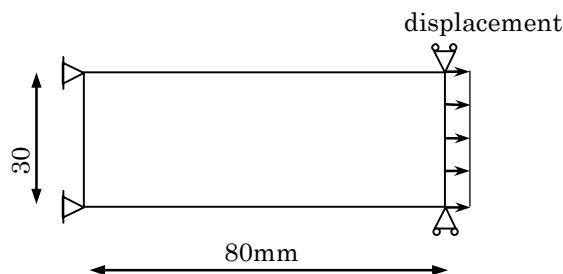
Figure 5. Analytical model.

4.1 Estimating procedure

The stress-strain relationship under tensile fatigue of PVA-ECC is estimated by applying finite element analysis. Cracks are modeled based on the concept of discrete crack, and the bridging stress-crack opening displacement under fatigue derived in chapter 2 is introduced by interface element.

Finite element model is shown in Figure 5, which refers to the measuring range of tensile strain of uniaxial direct tensile test (JSCE 2007). Analysis is conducted by using this model due to the following reasons although the size is different from the specimen of uniaxial tensile fatigue test in Figure 4.

- Cracks were observed only at the measuring range of tensile strain with small cross section area in the experiment.
- The process of cracking is not changed under uniaxial tension.

Element size is determined by referring to the intervals of cracks observed in the uniaxial tension test conducted by Kanda et al. (1998b), as minimum length of each element is about 1.5mm. Load is given by displacement. Crack initiates when axial stress reaches crack strength, and interface element is inserted into the whole cracking cross section, assuming steady state cracking. Then, the randomness of crack strength is considered based on the probability density function subjected to Gauss distribution.

In the fatigue analysis, the constitutive relation of interface element, the relationship between bridging stress and crack opening displacement, is deteriorated based on the apparent number of cycles.

Also, the reduction of crack strength under fatigue is defined in the following.

$$\frac{f_N}{f_1} = 1 - k_m \log(N) \tag{7}$$

where f_N=crack strength at N cycles; f_1=initial crack strength($=3\text{N/mm}^2$); and k_m=parameter

The value of k_m is 1/17, referring to fatigue design formulation of concrete (JSCE 2002).

4.2 Estimated results

4.2.1 Static analysis

The tensile stress-strain relationship under static loading is shown in Figure 6 (number of cycles=1. Figure 7 is the crack distribution when tensile strain equals to 0.001, 0.0015 and 0.002. From Figure 6 and 7, it is confirmed that multiple cracking property and the pseudo strain hardening behavior can be expressed in analysis. Tensile strain at tensile strength, ultimate tensile strain, reaches about 0.015. The similar value of ultimate tensile strain was obtained from uniaxial tensile test of PVA-ECC with the similar fiber properties and mix proportion. Therefore, it is shown that the tensile behavior of ECC can be estimated by bridging law and discrete crack model. On the other hand, the ultimate tensile strain observed in the test explained in chapter 3 was about 0.004, and the calculated relationship does not reproduce ultimate state. In experiments, the tensile strain capacity can be extremely poor in which initial defect and local volume fraction nearby cracks influence the multiple cracking property. In contrast, fibers and matrix exercise the performance ideally in analysis. This probably causes the difference of tensile strain capacity between analysis and experiment.

4.2.2 Fatigue analysis

The stress-strain relationships under tensile fatigue with variable number of cycles, 1, 10, 10^2, 10^3, 10^4 and 10^5, are shown in Figure 6. Here, softening behavior is not modeled, so that the slope in softening is assumed based on the static test conducted by Kanda et al. (1998b).

In Figure 6, tensile stress and ultimate tensile strain decrease when bridging stress deteriorates with the increase of number of cycles. Before 1,000 cycles, the pseudo strain hardening behavior is observed because maximum bridging stress is larger than crack strength. Also, the magnitude of tensile stress reduction is same rate as the reduction of crack strength because remarkable bridging stress degradation is not shown in pre-peak relationship in Figure 2. The increase of the number of ruptured fibers with the increase of number of cycles causes the reduction of maximum bridging stress. After 10,000 cycles ECC shows softening behavior without showing hardening behavior because tensile stress reaches maximum bridging stress at initial cracking. Figure 8 shows the maximum bridging stress-number of cycles relationship and the crack strength-number of cycles relationship. From this figure, the stress-strain relationship can be easily estimated.

Above results approximately corresponds to the multiple cracking property estimated by bridging stress degradation model in chapter 2. Critical number of cycles showing multiple cracking, estimated
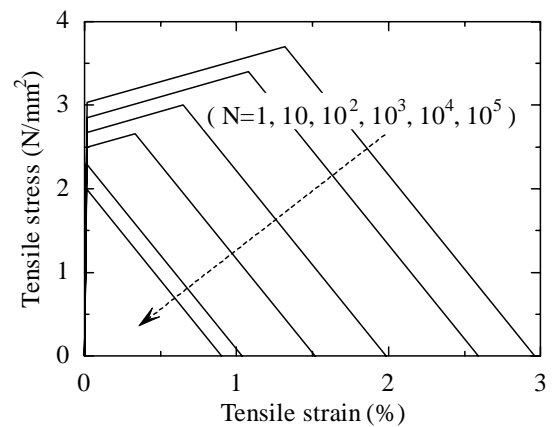
Figure 6. Tensile stress-strain relationship.

(a) ε_t=0.001
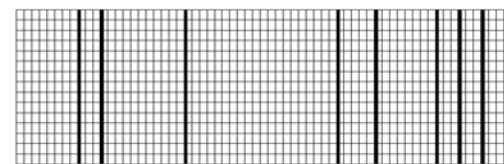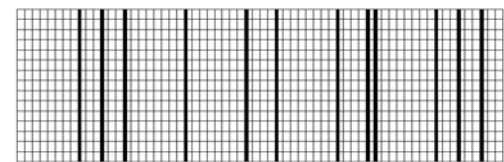
(b) ε_t=0.0015
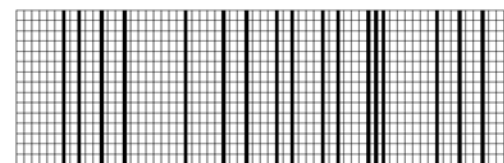
(c) ε_t=0.002

Figure 7. Crack distribution.
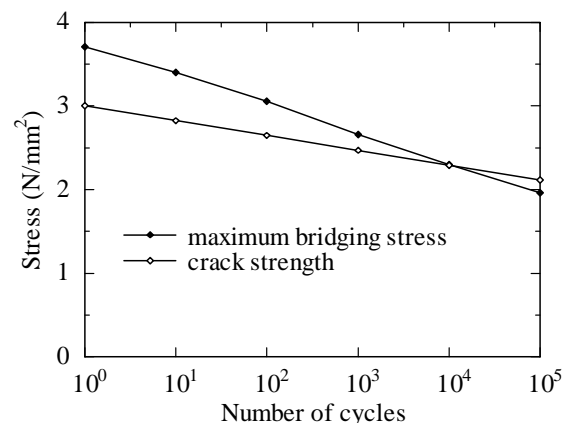
Figure 8. The evolution of maximum bridging stress and crack strength.

by the tensile stress-strain relationship, is 10,000 cycles, while that estimated in chapter 2 is 1,000 cycles. Although the limit showing multiple cracking is overestimated compared with in chapter 2 due to the difference of analytical object, it is easily estimated by the relationship between crack strength and maximum bridging stress.

The analytical result is compared with the uniaxial tensile fatigue test about the ratio between the tensile stress at N cycles, σ_N, and the value at initial cycle, σ_1, when the tensile strain equals to the focused value, 0.001, 0.0015 and 0.002. Figure 9 shows the relationship between the σ_N/σ_1 value and number of cycles. In the figure, analytical result agrees well with experimental one in all cases, and the criterion of fiber fatigue rupture defined in Equation 6 is proper relationship to estimate the degradation of bridging stress of PVA-ECC. When the evolution of the σ_N/σ_1 value focused on the difference of maximum tensile strain is seen, the slope tends to become steep with the increases of tensile strain in both analysis and experiment. This is because fiber fatigue rupture is promoted by increase of fiber pullout load which is caused by expansion of crack opening displacement, corresponding to the increase of tensile strain. Also, in all cases, the slope becomes large when number of cycles increases because fiber strength reduction promotes fiber fatigue rupture.

In real composites, the magnitude of the reduction of apparent fiber tensile strength change depends on the amount of deformation or slip of fibers, although Equation 6 is simply defined as a function of number of cycles. In this analysis, the crack opening displacements at focused tensile strains are similar each other because the difference of the prepared strain amplitudes of uniaxial tensile fatigue test is comparatively small, so that the criterion can reproduce the experiment under several tensile strains. Therefore, additional experiments under large tensile strain and the re-verification of the proposed model may be necessary.

5 CONCLUSIONS

This study developed the tensile stress-strain relationship of PVA-ECC under uniaxial fatigue tension. The fatigue degradation model of ECC was based on bridging stress degradation, and fiber fatigue rupture was considered as a degradation factor. The stress-strain relationship was obtained by applying the bridging stress-crack opening displacement relationship into finite element analysis as discrete crack model. The results obtained from this study are shown in the followings.

The bridging stress-crack opening displacement relationship under tensile fatigue was obtained by considering the change of micromechanical parameters in bridging law. As a result, it was suggested that multiple cracking behavior of ECC can be shown under fatigue loading before number of cycles reaches a certain critical value.

(a) ε_t=0.001

(b) ε_t=0.0015

(c) ε_t=0.002
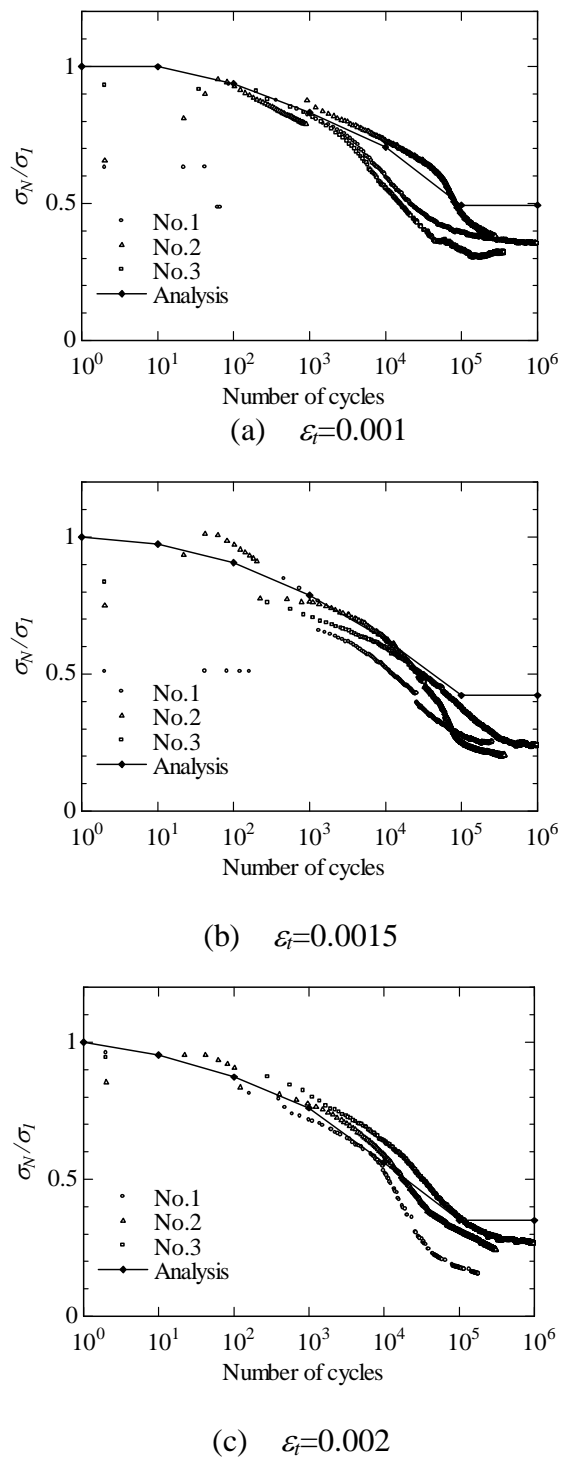
Figure 9. The σ_N/σ_1 value and number of cycles relationship.

The evolution of stress degradation obtained from the stress-strain relationship reproduced the reduction of bridging stress observed in the uniaxial tensile fatigue test of PVA-ECC. This means that the tensile constitutive law for fatigue analysis of ECC as members or structures is given.

For the future studies, the followings are considered.

To expand the fatigue mode including another degradation factor, fiber pullout, is necessary from the point of the development of fatigue model independent of the factor of bridging stress degradation.

To estimate the fatigue durability of ECC as members or structures by using the fatigue model proposed in this study.

REFERENCES

Japan Society of Civil Engineers. 2002. Standard specifications for concrete structures "Structural performance verification". (in Japanese)

Japan Society of Civil Engineers. 2007. Recommendations for design and construction of High Performance Fiber Reinforced Cement Composite with multiple fine cracks

Kanda, T. et al. 1998a. Interface property and apparent strength of high-strength hydrophilic fiber in cement matrix. *Journal of Materials in Civil Engineering*. 10(1): 5-13.

Kakuma, K. et al. 2009a. Estimation of stress-strain relation of ECC under uniaxial tensile fatigue. *Proceedings of Japan Concrete Institute*. 31(1): 277-282. (in Japanese)

Kakuma, K. et al. 2009b. Flexural fatigue analysis of PVA-ECC based on micromechanics approach. *International Conference on Computational Design in Engineering*.

Kanda, T. et al. 1998b. Material design and development of high-ductility composite reinforced with short random polyvinyl alcohol fiber. *Proceedings of Japan Concrete Institute*. 20(2): 229-234. (in Japanese)

Li, V. C. 1992. Post-crack scaling relation for fiber-reinforced cementitious composites, *Journal of Materials in Civil Engineering*. 4(1): 41-57.

Li, V. C. 1993. From micromechanics to structural engineering-the design of cementitious composites for civil engineering applications. *Journal of Structural Mechanics and Earthquake Engineering*. 10(2): 37-48.

Matsumoto, T. et al. 2003. Mechanisms of multiple cracking and fracture of DFRCC under fatigue flexure. *Journal of Advanced Concrete Technology*. 1(3): 299-306.

Matsumoto, T. et al. 2004. Effect of fiber fatigue rupture on bridging stress degradation in fiber reinforced cementitious composites. *Proceedings of FRAMCOS-5* (2): 653-660.

Mitamura, H. et al. 2006. Investigation for overlay reinforcement method on steel deck utilizing Engineered Cementitious Composites. *Journal of Materials, Concrete Structures and Pavements*. 62(2): 356-375. (in Japanese)